Journal of Zhejiang University-SCIENCE A (Applied Physics & Engineering)
ISSN 1673-565X (Print); ISSN 1862-1775 (Online)
www.zju.edu.cn/jzus; www.springerlink.com
E-mail: jzus@zju.edu.cn

Evaluation of the heat transfer performance of helical coils of non-circular tubes

Jundika C. KURNIA[1], Agus P. SASMITO[1], Arun S. MUJUMDAR[†‡1,2]

(*[1]Department of Mechanical Engineering, National University of Singapore, Singapore 117575, Singapore*)

(*[2]Mineral, Metal and Material Technology Centre, National University of Singapore, Singapore 117575, Singapore*)

[†]E-mail: mpeasm@nus.edu.sg

Received June 24, 2010; Revision accepted Nov. 15, 2010; Crosschecked Dec. 7, 2010

Abstract: This study addresses heat transfer performance of various configurations of coiled non-circular tubes, e.g., in-plane spiral ducts, helical spiral ducts, and conical spiral ducts. The laminar flow of a Newtonian fluid in helical coils made of square cross section tubes is simulated using the computational fluid dynamic approach. The effects of tube Reynolds number, fluid Prandtl number, coil diameter, etc., are quantified and discussed. Both constant wall temperature and constant heat flux conditions are simulated. The effect of in-plane coil versus a cylindrical design of constant coil, as well as a conical coil design is discussed. Results are compared with those for a straight square tube of the same length as that used to form the coils. Advantages and limitations of using coiled tubes are discussed in light of the numerical results.

Key words: Coil, Non-circular tube, Heat transfer performance, Mathematical model
doi:10.1631/jzus.A1000296 **Document code:** A **CLC number:** TK22

1 Introduction

Coiled tubes have been widely used in process industries due to their compactness, high heat transfer rate and ease of manufacture. They are commonly used as heat exchangers and chemical reactors. Other applications where the coiled tubes are considered and employed include rocket engines, fuel cell coolant channels, power plants, viscometers, and many other engineering applications. Aside from their industrial applications, transport phenomena in coiled ducts have also attracted much attention from engineering researchers. Secondary flow motion induced by the coil curvature, and complex temperature profile caused by helical torsion are among the more significant transport phenomena in coiled tubes.

Because of their importance in engineering applications, numerous studies have been conducted to investigate the heat transfer and flow characteristics inside coiled tubes. Among the first researchers in this field, Dean (1927a; 1927b) conducted a study of fluid flow inside a toroidal (in-plane) constant radius duct, and reported that circular tubes develop a secondary flow when the Dean number exceeds a critical value. Later, it was found that secondary flow can appear as one pair or two pairs depending on its Dean number (Joseph *et al.*, 1975; Masliyah, 1980; Dennis and Ng, 1982; Nandakumar and Masliyah, 1982). Joseph and Adler (1975) studied the effect of periodic laminar flow inside helical coiled tube and found that the secondary flow pattern depends on the relative strength of wall velocity and the velocity of flow through the tube. Dravid *et al.* (1971) numerically investigated the effect of secondary flow on the laminar heat transfer in helical coiled tube. They reported that the heat transfer coefficient undergoes a cyclic oscillation as the axial distance increases until the fully-developed flow is reached, after which the

[‡] Corresponding author

oscillation is damped out. Akiyama and Cheng (1974) reported a similar phenomenon, by numerically investigating the thermal entrance region in curved pipes with uniform heat flux. The effect of fluid properties (Kumar *et al.*, 2007; Shokouhmand and Salimpour, 2007a), non-Newtonian fluid (Norouzi *et al.*, 2009), curvature effect (Liou, 1992; Naphon and Suwagrai, 2007; Shokouhmand and Salimpour, 2007a; 2007b), cross section aspect ratio (Egner and Burmeister, 2005), Reynolds number (Liou, 1992; Kumar *et al.*, 2007; Shokouhmand and Salimpour, 2007a; 2007b), and longitudinal ribs/corrugated surface (Ko, 2006) on the heat transfer performance of coiled tubes have also been investigated. Similar to laminar flow, the turbulent flow inside coiled tubes has also attracted attention from engineering researchers. Several studies have been conducted on the turbulent flow behavior inside coiled tube (Rogers and Mayhew, 1964; Lin and Ebadian, 1997; Kaya and Teke, 2005). On the practical application of coiled tubes, few studies were designated to investigate the heat transfer performance of helical coil heat exchanger with helically crimped fins (Naphon, 2007), coiled flow inverter heat exchanger (Mandal *et al.*, 2010), tube in tube helically coiled heat exchanger (Kumar *et al.*, 2008), and spirally coiled finned-tube heat exchanger (Wongwises and Naphon, 2006). Moreover, Agrawal and Nigam (2001) investigated the application of coiled tubes as chemical reactors. In addition to the extensive numerical and experimental studies, reviews on the flow characteristic and heat transfer performance of a coiled tube and its potential applications have also been reported (Naphon and Wongwises, 2006; Vashisth *et al.*, 2008).

The majority of these studies were conducted to investigate fundamental transport phenomena occurring in the coiled circular tubes, and to develop correlations for the heat transfer coefficient. None has arrived at a definite conclusion on optimum design yet. It is therefore of interest to investigate heat transfer performance for various geometries of tubes made into coiled ducts and to seek optimum designs for practical applications.

This study investigates the heat transfer performance of coiled non-circular tubes with the aim to determine potential advantages and limitations of coiled noncircular tubes and provide design guidelines for their applications.

2 Mathematical model

2.1 Governing equations

Here, we consider incompressible laminar Newtonian fluid flow inside a helical coil with square cross section. The configuration of the coiled non-circular tubes and their cross section schematic are shown in Fig. 1. Both constant wall heat flux and constant wall temperature conditions are investigated. Since this work relates only to laminar flow, a precise numerical solution is adequate to simulate reality very closely. Conservation equations for mass, momentum, and energy for the flow inside the tubes are given by

$$\nabla \cdot \rho \boldsymbol{u} = 0, \tag{1}$$

$$\nabla \cdot \left(\rho \boldsymbol{u} \otimes \boldsymbol{u}\right) = -\nabla P + \nabla \cdot \left[\mu\left(\nabla \boldsymbol{u} + \left(\nabla \boldsymbol{u}\right)^{\mathrm{T}}\right)\right], \tag{2}$$

$$\rho c_{\mathrm{p}} \boldsymbol{u} \cdot \nabla T = k \nabla^2 T, \tag{3}$$

where ρ is the fluid density, $\boldsymbol{u}$ is the fluid velocity, P is the pressure, μ is the dynamic viscosity of the fluid, c_{p} is the specific heat of the fluid, k is the thermal conductivity, and T is the temperature.

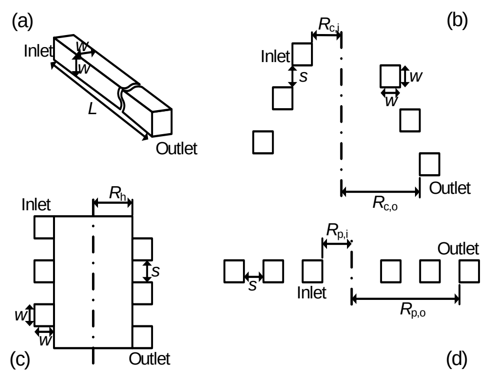

Fig. 1 Schematic representation of straight duct (a), conical spiral duct (b), helical spiral duct (c), and in-plane spiral duct (d)
w is the channel width, s is the space between channel, L is the length of the channel; and $R_{\mathrm{c,i}}$, $R_{\mathrm{c,o}}$, $R_{\mathrm{p,i}}$, and $R_{\mathrm{p,o}}$ are the inner and outer radii of conical and in-plane spiral, respectively

2.2 Constitutive relations

Two working fluids, air and water, are used in this study to investigate the effect of the Prandtl number. Thermo-physical properties of the fluids are generally given as functions of temperature.

The air properties are obtained as polynomial functions of temperature (Kays *et al.*, 2005). The air density is defined by

$$\rho_{\text{air}} = 1.076\times10^{-5}T^2 - 1.039\times10^{-2}T + 3.326, \quad (4)$$

while the air viscosity is given by

$$\begin{aligned}\mu_{\text{air}} &= 5.21\times10^{-15}T^3 - 4.077\times10^{-11}T^2 \\ &\quad + 7.039\times10^{-8}T + 9.19\times10^{-7}.\end{aligned} \quad (5)$$

The thermal conductivity of air is calculated from

$$\begin{aligned}k_{\text{air}} &= 4.084\times10^{-10}T^3 - 4.519\times10^{-7}T^2 \\ &\quad + 2.35\times10^{-4}T - 0.0147.\end{aligned} \quad (6)$$

The specific heat of air is defined as

$$\begin{aligned}c_{\text{p,air}} &= -4.67\times10^{-6}T^3 + 4.837\times10^{-3}T^2 \\ &\quad - 1.599T + 1175.\end{aligned} \quad (7)$$

The thermo-physical properties of water are defined as functions of temperature. The density, viscosity, thermal conductivity, and specific heat of water are given by (Kays *et al.*, 2005)

$$\rho_{\text{w}} = -3.570\times10^{-3}T^2 + 1.88T + 753.2, \quad (8)$$

$$\mu_{\text{w}} = 2.591\times10^{-5}\times10^{\frac{238.3}{T-143.2}}, \quad (9)$$

$$\begin{aligned}k_{\text{w}} &= -8.354\times10^{-6}T^2 \\ &\quad + 6.53\times10^{-3}T - 0.5981,\end{aligned} \quad (10)$$

$$c_{\text{p,w}}=4200. \quad (11)$$

The results will be discussed later in terms of the mixed mean temperature along the tubes, total heat rate, and figure of merit. The mixed mean temperature is given by (Kays *et al.*, 2005)

$$T_{\text{mean}} = \frac{1}{VA_{\text{c}}}\int_{A_{\text{c}}} T\boldsymbol{u}\,\mathrm{d}A_{\text{c}}, \quad (12)$$

where A_{c} is the cross section area of the channel, and V is the mean velocity given by (Kays *et al.*, 2005)

$$V = \frac{1}{A_{\text{c}}}\int_{A_{\text{c}}} \boldsymbol{u}\,\mathrm{d}A_{\text{c}}. \quad (13)$$

The total heat transfer rate, $\dot{Q}_{\text{total}}$, and figure of merit, F_{merit}, are defined as

$$\dot{Q}_{\text{total}} = \dot{m}c_p\left(T_{\text{mean},L} - T_{\text{mean},0}\right), \quad (14)$$

$$F_{\text{merit}} = \frac{\dot{Q}_{\text{total}}}{\Delta P}, \quad (15)$$

where $T_{\text{mean},L}$ and $T_{\text{mean},0}$ is the mixed mean temperature at the length L and at the channel inlet, respectively.

2.3 Boundary conditions

Boundary conditions for the fluid flow inside tubes are summarized as follows: inlet, $\boldsymbol{u}=\boldsymbol{u}_{\text{in}}$, $T=T_{\text{in}}$; outlet, $P=P_{\text{out}}$, $\boldsymbol{n}\times(k\nabla T)=0$; wall, $\boldsymbol{u}=0$, $T=T_{\text{wall}}$, or $\boldsymbol{n}\times(k\nabla T)=\dot{Q}_{\text{wall}}$. $\boldsymbol{n}$ is the normal vector, $\boldsymbol{u}_{\text{in}}$ is the inlet velocity which corresponds to Re=100, 500, and 1000 (0.156, 0.778, and 1.56 for air, and 0.01, 0.05, and 0.1 for water, respectively).

The values for these variables are summarized in Table 1.

Table 1 Base case and operating parameters

Parameter	Value
Temperature of the inlet, T_{in} (°C)	25
Wall temperature, T_{wall} (°C)	50
Channel width, w (m)	1×10^{-2}
Space between channel, s (m)	1×10^{-2}
Inner radius of in-plane spiral, $R_{\text{p,i}}$ (m)	2×10^{-2}
Outer radius of in-plane spiral, $R_{\text{p,o}}$ (m)	9×10^{-2}
Radius of helical spiral, R_{h} (m)	4×10^{-2}
Inner radius of in-plane spiral, $R_{\text{c,i}}$ (m)	2×10^{-2}
Outer radius of in-plane spiral, $R_{\text{c,o}}$ (m)	9×10^{-2}
Outlet pressure, P_{out} (gauge) (Pa)	0

3 Numerics

The computational domains (Fig. 2) were created in AutoCAD 2010 software. The commercial pre-processor software GAMBIT 2.3.16 was used for meshing, labeling boundary conditions, and determining the computational domain. Three different mesh sizes of 1×10^5, 2×10^5, and 6×10^5 were implemented and compared in terms of local pressure, velocities, and temperatures to ensure a mesh independent. We found that the mesh size of 2×10^5 gives about 1% deviation compared to that of 6×10^5; meanwhile, the results from the mesh size of 2×10^5 deviate up to 7% as compared to those from the finest one. Therefore, a mesh of around 2×10^5 elements was sufficient for the numerical investigation purposes: a fine structured mesh near the wall to resolve the boundary layer and an increasingly coarser mesh in the middle of the channel to reduce the computational cost.

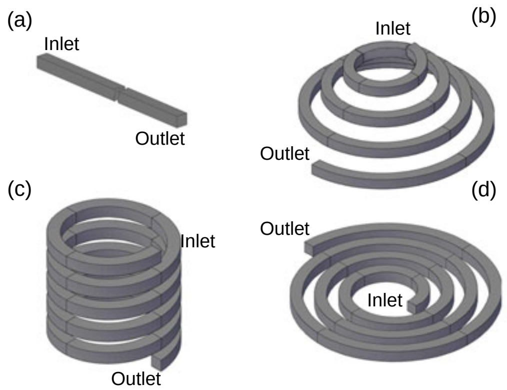

Fig. 2 Computational domain for straight duct (a), conical spiral duct (b), helical spiral duct (c), and in-plane spiral duct (d)

The mathematical model given by Eqs. (1)–(3), together with appropriate boundary condition and constitutive relations comprising five dependent variables, u, v, w, P, and T, was then solved by using commercial Finite Volume Solver Fluent 6.3.26 and user-defined functions (UDFs) written in C language to modify the thermo-physical properties of the fluid.

The numerical model was solved with the semi-implicit pressure-linked equation (SIMPLE) algorithm, first-order upwind discretization, and the algebraic multigrid (AMG) method. As an indication of the computational cost, it is noted that on average, around 200–500 iterations are needed for convergence criteria for all relative residuals of 10^{-6}. This takes 5–15 min on a workstation with a quad-core processor (1.8 GHz) and 8 GB of random-access memory (RAM).

4 Results and discussion

The numerical simulations were carried out for air and water at three different Reynolds numbers, i.e., 100, 500, and 1000, respectively (Table 2).

Table 2 Details of parameters for the simulations

Fluid	Inlet velocity, u_{in} (m/s)		
	Re=100	*Re*=500	*Re*=1000
Air	0.16	0.78	1.56
Water	9.03×10^{-3}	4.52×10^{-3}	9.03×10^{-2}
Fluid	Wall heat flux, Q_{wall} (W/m^2)		
	Re=100	*Re*=500	*Re*=1000
Air	9.8	47.6	88.3
Water	1838.8	5166.8	7359.8

This study examines four different non-circular tubes geometries, straight, conical spiral, helical spiral, and in-plane spiral ducts. As the convective heat transfer inside the tube is directly linked to the flow behavior, it is therefore of interest to investigate the flow pattern inside the tube. Many researchers (Dean, 1927a; 1927b; Joseph *et al.*, 1975; Masliyah, 1980; Dennis and Ng, 1982; Nandakumar and Masliyah, 1982) have shown that the presence of centrifugal force due to curvature will lead to a significant radial pressure gradient in the flow core region. In the proximity of the inner and outer walls of the curved tubes, however, the axial velocity and the centrifugal force will approach zero. Hence, to balance the momentum transport, secondary flows will appear (Vashisth *et al.*, 2008; Norouzi *et al.*, 2009). This is indeed the case, as can be seen in Fig. 3, where the secondary flow with higher velocities is generated in the outer walls of helical and spiral tubes. On closer inspection, in this particular Reynolds and Dean

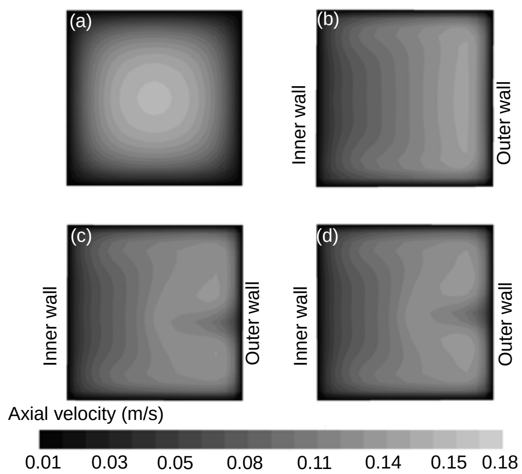

Fig. 3 Axial velocity (m/s) profile of air flow with constant wall temperature
(a) Straight duct; (b) Conical spiral duct; (c) Helical spiral duct; (d) In-plane spiral duct. L=50 cm, Re=1000

number, it was found that, in the conical spiral tube, the secondary flows appeared in one pair; whereas in helical and in-plane spiral, the secondary flows appeared in two pairs. Note that the secondary flows may change when the Reynolds and/or Dean number is changed (Joseph *et al.*, 1975; Masliyah, 1980; Dennis and Ng, 1982; Nandakumar and Masliyah, 1982).

As expected, the presence of secondary flow will affect the heat transfer performance. This can be inferred from Fig. 4, which presents temperature distribution over the cross sections of various tube designs for the constant wall temperature case. As can be seen, the temperature is lower along the outer wall region where the secondary flow appears. For the constant wall temperature case, a lower temperature means that more heat is dissipated, which is mirrored by a higher heat transfer rate. Moreover, the higher intensity of the secondary flow will lead to a higher heat transfer rate, as can be inferred from Fig. 4 and Fig. 5b for helical and in-plane spiral geometries.

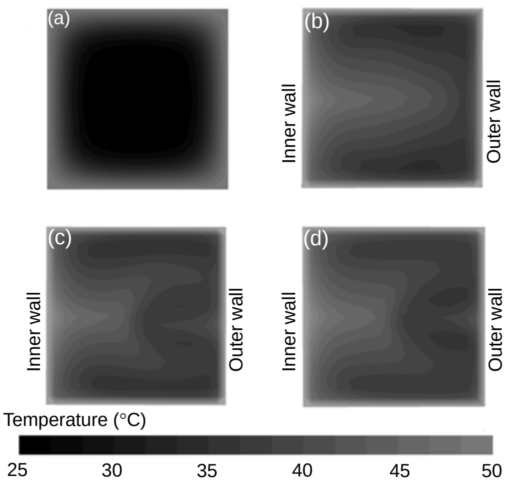

Fig. 4 Temperature distribution (°C) of air flow with constant wall temperature

(a) Straight duct; (b) Conical spiral duct; (c) Helical spiral duct; (d) In-plane spiral duct. L= 50 cm, Re=1000

Looking further into the mixed mean temperature variation along the tube length for both constant wall temperature and constant heat flux, it is noted that the helical and in-plane spiral tubes give the highest performance; whereas the straight tube gives the lowest heat transfer performance (Fig. 5). This heat transfer enhancement is mainly due to the secondary flows appearing at the outer wall. On closer inspection, it is noted that the heat transfer performance is not much different for the case of helical, conical spiral, and in-plane spiral; while for the straight tube, the performance difference is significant, especially for the case with a constant wall temperature (Fig. 5b). This can be adequately explained by the fact that a lower heat flux is taken away from the wall.

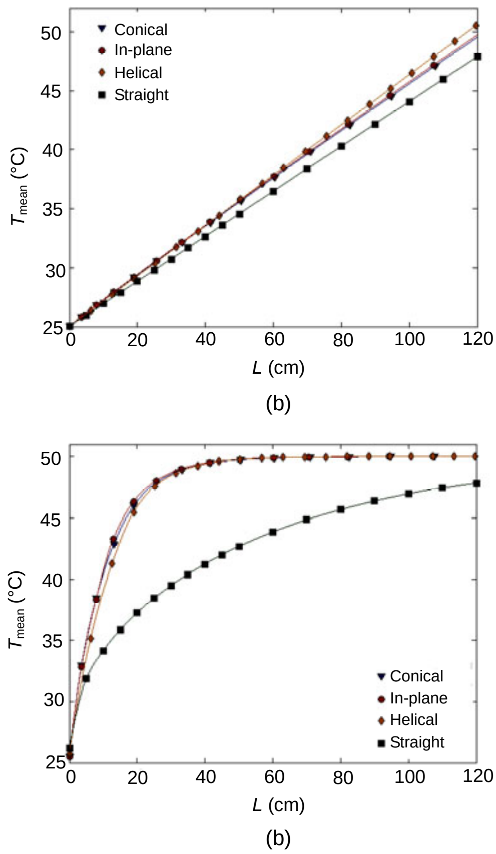

Fig. 5 Mixed mean temperature for the Reynolds number of 1000

(a) Constant heat flux; (b) Constant wall temperature

With respect to heat transfer performance, it is of interest to study the effect of Re and Pr, which are represented by inlet velocity and the fluid type (water and air, respectively). Hence, a total of 48 cases were simulated to represent various combinations of Re, Pr, and tube design. The summary of heat transfer performance for various cases is shown in Table 3. Here several features are apparently the foremost is that the helical tube yields the best heat transfer performance for constant wall heat flux case; whereas, for constant wall temperature, conical and in-plane spiral have better heat transfer rates. The straight tube, on the other hand, has the lowest heat transfer rate. Further, it is found that higher inlet velocity gives rise to a higher heat transfer rate. This is obvious in the heat transfer problem since higher velocity drives a higher mass flow rate and shorter residence time, which allows more heat to be removed. In addition, it is clear that water has a higher thermal conductivity and specific heat compared to air. Thus, as expected, water achieves higher heat transfer rates.

Table 3 Total heat transfer rate from channel wall to the fluid

Re	Geometries	Total heat transfer rate (J/s)			
		Constant Q_{wall}		Constant T_{wall}	
		Air	Water	Air	Water
100	Straight	0.47	88.15	0.37	83.46
	Conical	0.51	95.90	0.41	92.39
	Helical	0.55	103.96	0.40	91.39
	In-plane	0.51	96.25	0.41	92.39
500	Straight	2.28	247.88	2.11	242.15
	Conical	2.48	269.22	2.23	457.11
	Helical	2.68	291.84	2.19	461.95
	In-plane	2.49	270.20	2.23	457.11
1000	Straight	4.22	353.88	4.02	347.98
	Conical	4.58	383.99	4.54	851.06
	Helical	4.97	416.19	4.49	879.45
	In-plane	4.60	385.37	4.54	860.93

Q_{wall}: wall heat flux; T_{wall}: wall temperature

A further point of interest in this study is the parasitic load (pumping power) required to drive the flow, which is mirrored by the pressure drop in the tubes. As discussed earlier, the helical and spiral tubes give better heat transfer performance; however, this is not the case for pressure drop. The enhancement in heat transfer has to be paid by an increase in pressure drop/pumping power, as can be found in Table 4. Closer inspection reveals that the helical tube required the highest pressure drop compared to others, followed by in-plane spiral, conical spiral, and straight tubes. The pressure drop required by the helical tube was found to be up to around four times compared to the straight tube at a high *Re* (about 1000), and decreasing at a low *Re*. A possible explanation for the higher pressure drop is that the centrifugal force requires higher energy to overcome the friction along the tube and to generate secondary flows.

As regards the heat transfer performance and pressure drop in the system, the figure of merit concept is introduced to account for the effectiveness of heat transfer performance over pressure drop. Table 5 shows the figure of merit for various cases. It was found that, apart from the lowest heat transfer rate, the straight tube, interestingly, has the highest figure of merit among others. This is due to the fact that the straight tube requires the lowest pressure drop. The helical tube, on the other hand, has the lowest figure of merit, though it has the highest heat transfer performance due to its high pressure drop.

Table 4 Pressure drop along the channel

Re	Geometries	Pressure drop (Pa)			
		Constant Q_{wall}		Constant T_{wall}	
		Air	Water	Air	Water
100	Straight	1.08	2.08	1.12	1.85
	Conical	1.43	3.04	1.49	2.68
	Helical	1.59	3.32	1.63	2.96
	In-plane	1.41	3.00	1.47	2.64
500	Straight	5.90	11.75	6.56	11.10
	Conical	11.67	28.05	11.48	24.93
	Helical	13.49	31.89	13.92	28.19
	In-plane	11.80	28.24	11.65	24.69
1000	Straight	13.10	26.43	13.35	25.38
	Conical	31.98	77.20	33.42	68.50
	Helical	36.78	88.48	38.24	77.83
	In-plane	32.23	78.46	33.71	69.39

Q_{wall}: wall heat flux; T_{wall}: wall temperature

Table 5 Figure of merit for various channel configuration

Re	Geometries	Figure of merit			
		Constant Q_{wall}		Constant T_{wall}	
		Air	Water	Air	Water
100	Straight	0.43	42.38	0.33	45.18
	Conical	0.36	31.51	0.28	34.48
	Helical	0.35	31.32	0.24	30.82
	In-plane	0.37	33.08	0.25	33.91
500	Straight	0.39	21.10	0.32	21.81
	Conical	0.21	9.60	0.19	18.34
	Helical	0.20	9.15	0.16	16.39
	In-plane	0.22	10.04	0.18	18.66
1000	Straight	0.32	13.39	0.30	13.71
	Conical	0.14	4.97	0.14	12.42
	Helical	0.14	4.70	0.12	11.30
	In-plane	0.15	5.14	0.13	12.78

Q_{wall}: wall heat flux; T_{wall}: wall temperature

When designing a heat exchanger, however, careful balance into consideration has to be taken between compactness/size, performance, and pumping power. If the compactness and performance is of interest, one can consider a helical or spiral tube to be used for heat exchanger. For example, a spiral tube could be used for a compact heat exchanger in process industry, a helical coil for chemical reactor, and an in-plane spiral for coolant plate in a fuel cell stack.

5 Conclusions

A computational study has been conducted to investigate the heat transfer performance of coiled non-circular ducts. Three configurations—conical, helical, and in-plane spiral—have been investigated and their performances are compared to the straight duct in terms of a figure of merit. It is found that even though coiled ducts give higher heat transfer rates, they also impose a higher pressure drop penalty. As a result, the figure of merit of the coiled ducts is lower than that of the straight duct. However, for an operation where space is limited and pumping power is not an issue, the coiled duct can be a desired choice. Additional research is ongoing to evaluate other parameters.

References

Agrawal, S., Nigam, K.D.P., 2001. Modeling of coiled tubular chemical reactor. *Chemical Engineering Journal*, **84**(3): 437-444. [doi:10.1016/S1385-8947(00)00370-3]

Akiyama, M., Cheng, K.C., 1974. Graetz problem in curved pipes with uniform wall heat flux. *Applied Scientific Research*, **29**(1):401-418. [doi:10.1007/BF00384162]

Dean, W.R., 1927a. Note on the motion of fluid in a curved pipe. *Philosophical Magazine*, **4**(20):208-223.

Dean, W.R., 1927b. The stream-line motion of fluid in a curved pipe. *Philosophical Magazine*, **5**(7):208-223.

Dennis, S.C.R., Ng, M., 1982. Dual solutions for steady laminar flow through a curved tube. *The Quarterly Journal of Mechanics and Applied Mathematics*, **35**(3): 305-324. [doi:10.1093/qjmam/35.3.305]

Dravid, A.N., Smith, K.A., Merril, E.W., Brian, P.L.T., 1971. Effect of secondary fluid motion on laminar flow heat transfer in helically coiled tubes. *AIChE Journal*, **17**(5): 1114-1122. [doi:10.1002/aic.690170517]

Egner, M.W., Burmeister, L.C., 2005. Heat transfer for laminar flow in spiral ducts of rectangular cross section. *Journal of Heat Transfer*, **127**(3):352-356. [doi:10.1115/1.1857950]

Joseph, B., Adler, R.J., 1975. Numerical treatment of laminar flow in helically coiled tubes of square cross section. Part II: Oscillating helically coiled tubes. *AIChE Journal*, **21**(5):974-979. [doi:10.1002/aic.690210520]

Joseph, B., Smith, E.P., Adler, R.J., 1975. Numerical treatment of laminar flow in helically coiled tubes of square cross section part I: Stationary helically coiled tubes. *AIChE Journal*, **21**(5):965-974. [doi:10.1002/aic.690210519]

Kaya, O., Teke, I., 2005. Turbulent forced convection in helically coiled square duct with one uniform temperature and three adiabatic walls. *Heat and Mass Transfer*, **42**(2):129-137. [doi:10.1007/s00231-005-0656-3]

Kays, W., Crawford, M., Weigand, B., 2005. Convective Heat and Mass Transport (4th Ed.). McGraw Hill, Singapore.

Ko, T.H., 2006. A numerical study on entropy generation and optimization for laminar forced convection in a rectangular curved duct with longitudinal ribs. *International Journal of Thermal Sciences*, **45**(11):1113-1125. [doi:10.1016/j.ijthermalsci.2006.03.003]

Kumar, V., Gupta, P., Nigam, K.D.P., 2007. Fluid flow and heat transfer in curved tubes with temperature-dependent properties. *Industrial and Engineering Chemistry Research*, **46**(10):3226-3236. [doi:10.1021/ie0608399]

Kumar, V., Faizee, B., Mridha, M., Nigam, K.D.P., 2008. Numerical studies of a tube-in-tube helically coiled heat exchanger. *Chemical Engineering and Processing Process Intensification*, **47**(12):2287-2295. [doi:10.1016/j.cep.2008.01.001]

Lin, C.X., Ebadian, M.A., 1997. Developing turbulent convective heat transfer in helical pipes. *International Journal of Heat and Mass Transfer*, **40**(16):3861-3873. [doi:10.1016/S0017-9310(97)00042-2]

Liou, T.M., 1992. Flow visualization and LDV measurement of fully developed laminar flow in helically coiled tubes. *Experiments in Fluids*, **13**(5):332-338. [doi:10.1007/BF00209507]

Mandal, M.M., Kumar, V., Nigam, K.D.P., 2010. Augmentation of heat transfer performance in coiled flow inverter vis-à-vis conventional heat exchanger. *Chemical Engineering Science*, **65**(2):999-1007. [doi:10.1016/j.ces.2009.09.053]

Masliyah, J.C., 1980. On laminar flow in curved semicircular ducts. *Journal of Fluid Mechanics*, **99**(3):469-479. [doi:10.1017/S0022112080000717]

Nandakumar, K., Masliyah, J.C., 1982. Bifurcation in steady laminar flow through curved tubes. *Journal of Fluid Mechanics*, **119**:475-490. [doi:10.1017/S002211208200144X]

Naphon, P., 2007. Thermal performance and pressure drop of the helical-coil heat exchangers with and without helically crimped fins. *International Communications in Heat and Mass Transfer*, **34**(3):321-330. [doi:10.1016/j.ijheatmasstransfer.2006.08.002]

Naphon, P., Wongwises, S., 2006. A review of flow and heat transfer characteristics in curved tubes. *Renewable and Sustainable Energy Reviews*, **10**(5):463-490. [doi:10.1016/j.rser.2004.09.014]

Naphon, P., Suwagrai, J., 2007. Effect of curvature ratio on the heat transfer and flow developments in the horizontal spirally coiled tubes. *International Journal of Heat and Mass Transfer*, **50**(3-4):444-451. [doi:10.1016/j.ijheatmasstransfer.2006.08.002]

Norouzi, M., Kayhani, M.H., Nobari, M.R.H., Demneh, M.K., 2009. Convective heat transfer of viscoelastic flow in a curved duct. *World Academy of Science, Engineering and Technology*, **56**:327-333. [doi:10.1007/s00231-010-0641-3]

Rogers, G.F.C., Mayhew, Y.R., 1964. Heat transfer and pressure loss in helically coiled tubes with turbulent flow. *International Journal of Heat and Mass Transfer*, **7**(11):1207-1216. [doi:10.1016/0017-9310(64)90062-6]

Shokouhmand, H., Salimpour, M.R., 2007a. Optimal Reynolds number of laminar forced convection in a helical tube subjected to uniform wall temperature. *International Communications in Heat and Mass Transfer*, **34**(6): 753-761. [doi:10.1016/j.icheatmasstransfer.2007.02.010]

Shokouhmand, H., Salimpour, M.R., 2007b. Entropy generation analysis of fully developed laminar forced convection in a helical tube with uniform wall temperature. *Heat and Mass Transfer*, **44**(2):213-220. [doi:10.1007/s00231-007-0235-x]

Vashisth, S., Kumar, V., Nigam, K.D.P., 2008. A review on the potential applications of curved geometries in process industry. *Industrial and Engineering Chemistry Research*, **47**(10):3291-3337. [doi:10.1021/ie701760h]

Wongwises, S., Naphon, P., 2006. Heat transfer characteristics of a spirally coiled, finned-tube heat exchanger under dry-surface conditions. *Heat Transfer Engineering*, **27**(1): 25-34. [doi:10.1080/01457630500341698]